MODELING COUPLING EFFECTS IN CORD–RUBBER COMPOSITE STRUCTURES

Article · January 2007

CITATIONS
0

READS
112

3 authors, including:

Hedi Hassis
École Nationale d'Ingénieurs de Tunis
62 PUBLICATIONS **282** CITATIONS
SEE PROFILE

Saber El Arem
Ecole Nationale Supérieure d'Arts et Métiers
29 PUBLICATIONS **221** CITATIONS
SEE PROFILE

JP Journal of Solids and Structures
Volume 1, Issue 3, 2007, Pages 217-236
This paper is available online at http://www.pphmj.com

MODELING COUPLING EFFECTS IN CORD-RUBBER COMPOSITE STRUCTURES

HEDI HASSIS, SABER EL AREM and RAMANA M. PIDAPARTI*

Ecole Nationale d'Ingénieurs de Tunis
B.P. 37 Le belvédère 1002 Tunis, Tunisia

*Department of Mechanical Engineering
Virginia Commonwealth University
Richmond, VA 23284, U. S. A.

Abstract

An analytical model is developed to study the coupling effects in cord-rubber composite materials. The analytical model takes into account the mismatch of stiffness between the cords and the rubber matrix material, and the twist-extension coupling. The transverse deformation, i.e., normal to the cords direction is based on the normal modes of a special system which describes the orthotropic and the coupling behaviour of cord-rubber composites. The equations of motion for the cord-composite plates are derived using the principle of virtual work. Results of deformation and stresses are obtained for some typical cord-rubber composite plates and are compared to the existing solutions. The results presented illustrate that the coupling effects are significant for non-symmetrical cord orientations.

1. Introduction

Cord-reinforced rubber composite structures are being used in pneumatic tires, belt structures, and various military components. The combination of the cords and rubber material is especially effective when the composite material needs to be strong in extension in the cord direction, but also needs to be flexible in the plane perpendicular to the

Keywords and phrases: cord, composite, warping, coupling.

Received November 16, 2007

cords. Several authors treated the cord-composite plate structures from simple homogeneous models and a limited sophisticated representation. The analytical models representing the cord-composites are briefly described below.

Gough [3] and Tangaro [15] presented a homogeneous model, in which the system of the two materials is considered as an orthotropic composite material with the following mechanical properties

$$E_1 = c_1 E_c \eta_c + E_m(1 - \eta_c) \tag{1a}$$

$$E_2 = \frac{4E_m(1 - \eta_c)[c_1 E_c \eta_c + E_m(1 - \eta_c)]}{3E_c \eta_c + 4E_m(1 - \eta_c)} \tag{1b}$$

$$G_{12} = G_m(1 - \eta_c) \tag{1c}$$

$$\nu_{12} = 0.25; \quad \nu_{21} = \nu_{12} \frac{E_2}{E_1}, \tag{1d}$$

where E_1 and E_2 are the Young modulus in the x_1 and x_2 directions, respectively, ν_{12} is the Poisson ratio for transverse strain in the x_2 direction when stressed in the x_1 direction, and G_{12} is the shear modulus. The constants E_c and E_m are the Young modulus of the cord and the matrix, respectively, and η is the cord volume fraction. The constant c_1 is a coefficient defined by Gough [3] and Tangaro [15] and G_m is the shear modulus of the matrix. Later, Akasaka and Hirano [1] presented a simplified homogeneous orthotropic model with the following mechanical properties,

$$E_1 = c_1 E_c \eta_c \tag{2a}$$

$$E_2 = \frac{4E_m}{3} \tag{2b}$$

$$G_{12} = G_m \tag{2c}$$

$$\nu_{12} = 0.25; \quad \nu_{21} = 0. \tag{2d}$$

When the cord composite is modeled as a homogeneous orthotropic plate, a part of the mechanical response of the cord is neglected, which include,

- the twist-extension coupling behaviour

- the exact distribution of the cords in the cord-rubber layer (knowing that for the cord-matrix plate, the cords are all evenly spaced at specified heights through the plate's thickness).

Also for the homogeneous orthotropic plate, it is necessary to give the global behaviour for each plate's composition: spacing between cords, number of cord layer, position of each layer etc.

Shield and Costello [2, 12-14] presented the mechanical properties of cords and the coupling coefficient between extension and twist. Shield and Costello [13, 14] presented an elasticity approach and an energy approach leading to a combination of a 2D formulation (on the plane ω) associated to the matrix and 1-D formulation associate to the cords in the x_1 direction. The elasticity approach was not based on a rigorous formulation leading to uncompleted equilibrium equations, mainly the effect of non-symmetrical cord's position, section or mechanical properties. In the work of Shield and Costello, the Kirchhoff displacement is used and the effect of non-symmetrical reinforcement is not considered. The boundary conditions are not developed. Recently, Paris and Costello [7] analyzed the cord composite cylindrical shells. The differential equations were found for a shell with a single ply of uniformly spaced cords with the cord axes parallel to the shell axis.

Attempts have been made to study the behaviour of cord rubber composites by finite element methods as a complement to the experimental and analytical methods. Pidaparti, Yang and Soedel [10] studied the mechanical and fracture behaviour of single-ply cord rubber composites. The effects of orthotropic behaviour of cords, cords re-orientation, bimodulus behaviour, and the large deformation of the rubber material were considered in their finite element formulation. The bending behaviour and the combined tension and torsion behaviour of cord rubber laminates were investigated by Pidaparti et al. [8, 11] and found good agreement to the experimental data when the extension-twist coupling was considered. Recently, Kocak and Pidaparti [5] developed a 3D micro-mechanics model by treating the cord as a three-dimensional beam element along with a solid finite element for the rubber material to study the load deformation characteristics of cord-rubber composites.

A two-dimensional (2D) mechanical model based on the different mechanical properties of each constituent material in cord-rubber composites, and in which the one-dimensional properties of the cords are considered in an equivalent 2D model was presented by Hassis et al. (in press). The approach of Hassis and Pidaparti [4] gives more possibilities for combining the two different materials without any more experimental tests for each kind of composition and position of the cords.

A general formulation is developed representing the extension, the twist and the bending phenomena, and presented in this study. The possibility of a non-symmetrical cord's reinforcement in cord-rubber composites is also considered. The present model is based on the schematic representation as shown in Figure 1.

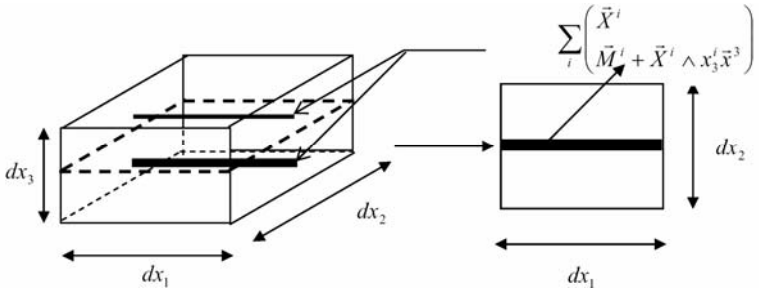

(a) Multiphase elementary volume (b) Multiphase elementary surface

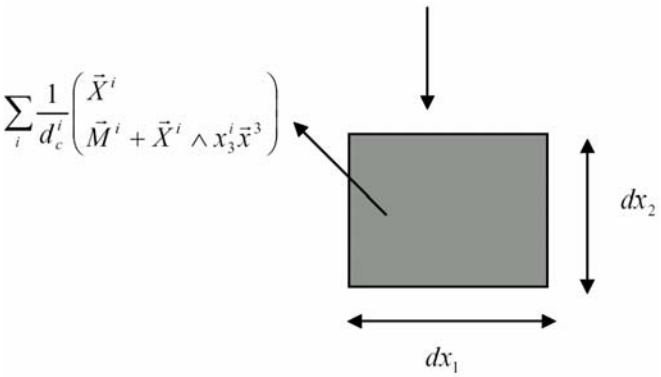

(c) Multiphase distributed elementary surface

Figure 1. A schematic representation of modeling cord-rubber composites.

The internal force tensors take the following expression when it is written in the mid-plane of the elementary volume of a cord-rubber composite unit cell as

$$\sum_i \begin{pmatrix} \vec{X}^i \\ \vec{M}^i + \vec{X}^i \wedge x_3^i \vec{x}^3 \end{pmatrix}, \tag{3}$$

where x_3^i is the cord's height through the plate's thickness. It is assumed that the cord is able to carry an axial force N_c, a twisting moment C_c and a bending moment M_c. The rubber matrix is assumed as a homogeneous isotropic material characterized by the membrane tensor, N_m, the moment tensor, M_m, and the shear stress resultant, T_m. Based on this model, the equilibrium equations are derived as,

$$\text{on } \omega \quad \begin{cases} divN_m + \sum_i div\left(\frac{N_c^i}{d_c^i}\vec{x}^1 \otimes \vec{x}^1\right) + \vec{F}_\omega = \vec{0} \\ divM_m - \vec{T}_m + \sum_i div\left(\left[\frac{N_c^i x_3^i}{d_c^i} + \frac{M_c^i}{d_c^i}\right]\vec{x}^1 \otimes \vec{x}^1 - \frac{C_c^i}{d_c^i}\vec{x}^2 \otimes \vec{x}^1\right) = \vec{0} \\ div\vec{T}_m + F^3 = 0. \end{cases} \tag{4}$$

2. Cord and Matrix Behaviour

A simple cord consisting of many strands, is represented by a central strand with radius R_i and n helical twists defined by the helix angle α and the radius R_0 (as shown in Figure 2). The cord is assumed to be able to carry an axial force N_c, a twisting moment C_c and a bending moment M_c. The cord behaviour is defined by the following relationship for a simple strand with helix angle α similar to the Shield and Costello [2, 12-14].

$$N_c = A_c E_c[c_1\varepsilon_{11} + c_2 R\tau] \tag{5a}$$

$$C_c = E_c R[c_3\varepsilon_{11} + c_4 R\tau] \tag{5b}$$

$$M_c = E_c R^4[c_5\kappa], \tag{5c}$$

where E_c is the modulus of elasticity of the cord material, $R = R_i + 2R_0$ (see Figure 2) is the radius of the cord, ε_{11} is the axial strain, κ is curvature and τ is the twist strain. The coefficient $c_1 - c_4$ are the cord constants defined by Shield and Costello [2, 12-14].

The matrix is considered as a homogeneous isotropic material characterized by the membrane tensor, N_m, the moment tensor, M_m, and the shear stress resultant, T_m, defined by the following constitutive relationships as,

$$N_m = D_2[(1-\nu_m)\underline{\underline{\gamma}} + \nu_m Tr(\underline{\underline{\gamma}})\underline{\underline{1}}]$$

$$M_m = D_1[(1-\nu_m)\underline{\underline{\chi}} + \nu_m Tr(\underline{\underline{\chi}})\underline{\underline{1}}]$$

$$T_m = D_3[(\vec{\beta} + \vec{\nabla}u_3)], \tag{6a}$$

where $\underline{\underline{\gamma}}$ is the membrane strain tensor, $\underline{\underline{\chi}}$ is the curvature tensor, and $\underline{\underline{1}}$ is the metric tensor. D_1, D_2 and D_3 are respectively the membrane, the flexural and the shear stiffness defined as

$$D_1 = \frac{E_m h^3}{12(1-\nu_m^2)}; \quad D_2 = \frac{E_m h}{(1-\nu_m^2)}; \quad D_3 = \frac{E_m h}{2(1+\nu_m)}, \tag{6b}$$

where E_m is the modulus of elasticity of the matrix, ν_m is the Poisson coefficient of the matrix, and h is the thickness of the plate.

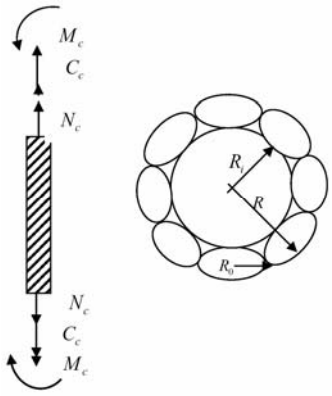

Figure 2. Loading and geometry of a simple strand of the cord.

3. Special Warping Model

As compared to rigid matrix composites, cord-rubber composites have the following features:

• the steel cord-rubber composites have a characteristic large stiffness ratio mismatch: the stiffness ratio, E_c/E_m, can range from 58 for vulcanized rubber to between 3000-50000 for synthetic rubber. With this large mismatch between the moduli, the shear and the warping cannot be ignored for most situations;

• the mechanical behaviour in the cord direction is much different as compared to the transverse direction (perpendicular to the cords);

• cord-rubber composites exhibits coupling between the tension and twisting due to twisted nature of the cords.

Let us consider the following equivalent system as a model, to describe the cinematic behaviour of the normal cord, for the cord-rubber composite plates (Figure 3).

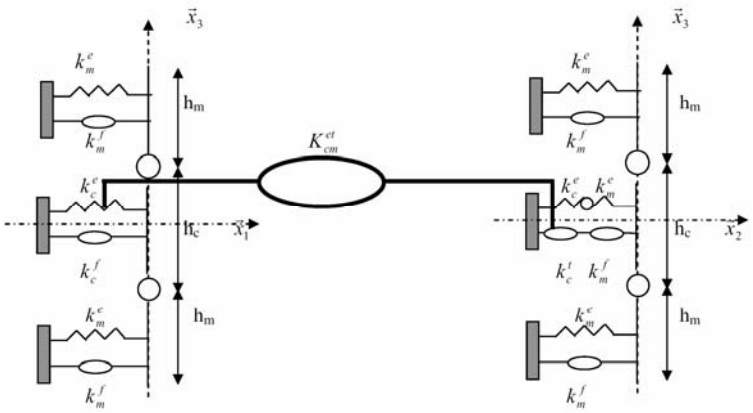

Figure 3. Mechanical system associated to the normal fiber, used in the special warping model.

Here $\vec{x}_1$ is the cord reinforcement direction, the motion of the normal fiber in the $(\vec{x}_1, \vec{x}_3)$ plane is considered as linear for each homogeneous layer. For the cord layer, the twist extension coupling is taken into account by the stiffness spring but with specific K_{cm}^{et}.

The motion of the normal fiber in the $(\vec{x}_2, \vec{x}_3)$ plane is considered as linear for each homogeneous layer. For the cord layer, and because of coexistence between the cord and the matrix, two springs, which disposed in series, are considered. The twist extension coupling is taken into account by the stiffness spring but with specific K_{cm}^{et}. The normal modes associated to the system defined by Figure 3 are calculated and considered as a complete base to any function described on the cord-matrix system. As an example, and for one layer of a cord-rubber system, Figure 5 shows the first eight in-plane transverse modes respectively in the $(\vec{x}_1, \vec{x}_3)$ and in the $(\vec{x}_2, \vec{x}_3)$ planes. The number of modes used depends on the order of the theory needed.

3.1. Displacement field

Considering the previous remarks, the following displacement fields are used to derive a special warping theory for the cord-rubber composite plates as

$$\vec{U} = \begin{cases} \begin{bmatrix} U_1(x^1, x^2, x^3) \\ U_2(x^1, x^2, x^3) \end{bmatrix} = u_\omega^n(x^1, x^2) \begin{bmatrix} \phi_1^n(x^3) \\ \phi_2^n(x^3) \end{bmatrix} \\ U_3(x^1, x^2, x^3) = u_3^k(x^1, x^2)\Phi^k(x^3) \end{cases} \tag{7}$$

(ϕ_1^n, ϕ_2^n) are the components of the in-plane transverse nth mode in the x_1 direction and in the x_2 direction, respectively. Φ^k is the longitudinal kth mode associated to the system described in Figure 3.

This displacement fields includes:

- both in-plane and out-plane deformation modes;

- the orthotropic behaviour of the plate;

- the extension-twist coupling of the cord.

3.2. Strain tensor

For the displacement field defined by equation (7), the following relations are obtained

$$\varepsilon_{11} = u_{\omega,1}^n \phi_1^n$$

$$\varepsilon_{22} = u^n_{\omega,2}\phi^n_2$$

$$2\varepsilon_{12} = u^n_{\omega,2}\phi^n_1 + u^n_{\omega,1}\phi^n_2$$

$$2\varepsilon_{13} = u^n_{\omega}\phi^n_{,3} + u^k_{3,1}\Phi^k$$

$$2\varepsilon_{23} = u^n_{\omega}\phi^n_{2,3} + u^k_{3,2}\Phi^k$$

$$\varepsilon_{33} = u^k_3\Phi^k_{,3}. \tag{8}$$

3.3. Equilibrium equations

The governing equations pertinent to this model are derived using the principle of virtual works. The internal virtual works is

$$W_i = -\int_\omega \int_{-\frac{h}{2}}^{\frac{h}{2}} \sigma^{\alpha\beta}\varepsilon_{\alpha\beta}dx^3d\omega - \int_\omega \int_{-\frac{h}{2}}^{\frac{h}{2}} 2\sigma^{\alpha 3}\varepsilon_{\alpha 3}dx^3d\omega - \int_\omega \int_{-\frac{h}{2}}^{\frac{h}{2}} \sigma^{33}\varepsilon_{33}dx^3d\omega$$

$$= -\int_\omega \int_{-\frac{h}{2}}^{\frac{h}{2}} \sigma^{\alpha\beta}u^n_{\omega,\alpha}\phi^n_\beta dx^3d\omega - \int_\omega \int_{-\frac{h}{2}}^{\frac{h}{2}} \sigma^{\alpha 3}[u^n_\omega\phi^n_{\alpha,3} + u_{3,\alpha}\Phi^k]dx^3d\omega$$

$$- \int_\omega \int_{-\frac{h}{2}}^{\frac{h}{2}} \sigma^{33}u^k_3\Phi^k_{,3}dx^3d\omega. \tag{9}$$

The expression of the internal virtual works becomes after integration by parts, and deriving the stress resultants, defined by (11)

$$W_i = -\int_\omega \overline{P}^\alpha_n u^n_{\omega,\alpha}d\omega - \int_\omega [\overline{Q}^\alpha u^n_\omega + \overline{S}^\alpha u_{3,\alpha}]d\omega - \int_\omega R_k u^k_3 d\omega$$

$$= \int_\omega \overline{P}^\alpha_{n,\alpha}u^n_\omega d\omega - \int_\omega [\overline{Q}^\alpha u^n_\omega - \overline{S}^\alpha_{,\alpha}u_3]d\omega - \int_\omega \overline{R}_k u^k_3 d\omega$$

$$- \int_{\partial\omega} \overline{P}^\alpha_n u^n_\omega \nu_\alpha d\Gamma - \int_{\partial\omega} \overline{S}^\alpha \nu_\alpha u_3 d\Gamma \tag{10}$$

with

$$\overline{P}^\alpha_n = \int_{-\frac{h}{2}}^{\frac{h}{2}} \sigma^{\alpha\beta}\phi^n_\beta dx^3; \quad \overline{S}^\alpha_k = \int_{-\frac{h}{2}}^{\frac{h}{2}} \sigma^{\alpha 3}\Phi^k dx^3;$$

$$\overline{Q}_n = \int_{-\frac{h}{2}}^{\frac{h}{2}} \sigma^{\alpha 3}\phi^n_{\alpha,3}dx^3; \quad \overline{R}_k = \int_{-\frac{h}{2}}^{\frac{h}{2}} \sigma^{33}\Phi^k_{,3}dx^3. \tag{11}$$

The external virtual work is (for the volume and surface densities) is

$$W_e = \int_{\omega}\int_{-\frac{h}{2}}^{\frac{h}{2}} [f_v^{\alpha}\phi_{\alpha}^{n}u_{\omega}^{n} + f_v^{3}\Phi^{k}u_3^{k}]dx^3 d\omega + \int_{\partial\omega}\int_{-\frac{h}{2}}^{\frac{h}{2}} [f_s^{\alpha}\phi_{\alpha}^{n}u_{\omega}^{n} + f_s^{3}\Phi^{k}u_3^{k}]dx^3 d\Gamma$$

$$= \int_{\omega} [F_v^{\omega}u_{\omega}^{n} + F_v^{3}u_3^{k}]d\omega + \int_{\partial\omega} [F_s^{\omega}u_{\omega}^{n} + F_s^{3}u_3^{k}]d\Gamma \tag{12}$$

with

$$F_v^{\omega} = \int_{-\frac{h}{2}}^{\frac{h}{2}} f_v^{\alpha}\phi_{\alpha}^{n}dx^3;\ F_v^{3} = \int_{-\frac{h}{2}}^{\frac{h}{2}} f_v^{3}\Phi^{k}dx^3;$$

$$F_s^{\omega} = \int_{-\frac{h}{2}}^{\frac{h}{2}} f_s^{\alpha}\phi_{\alpha}^{n}dx^3;\ F_s^{3} = \int_{-\frac{h}{2}}^{\frac{h}{2}} f_s^{3}\Phi^{k}dx^3. \tag{13}$$

The application of the virtual work leads to the following equilibrium equations and boundary conditions.

$$\text{on } \omega \quad \begin{cases} \overline{P}_{n,\alpha}^{\alpha} - \overline{Q}_n + F_v^{\omega} = 0 \\ \overline{S}_{k,\alpha}^{\alpha} - \overline{R}_k + F_v^{3} = 0 \end{cases} \tag{14}$$

$$\text{on } \partial\omega \quad \begin{cases} -\overline{P}_n^{\alpha} - \overline{Q}_n + F_s^{\omega} = 0 \\ -\overline{S}^{\alpha}\nu_{\alpha} + F_s^{3} = 0. \end{cases} \tag{15}$$

4. Results and Discussion

To demonstrate the present general analytical formulation for cord-composite plates illustrating the coupling effects, the example of a simply supported plate (with various cases of cord layer positions in the plate) is considered. The mechanical properties of the cords are taken from Shield and Costello [13-14] and given as,

E_c = 200Gpa; ν_c = 0.25; α = 81.4 deg; R_i = 0.15mm; 6 outer wires with radii R_0 = 0.14mm; Cord radius R = 0.43mm; c_1 = 0.967; c_2 = 0.0828; c_1 = 0.187; c_1 = 0.0723; η_c = 0.0116%.

The plate is subjected to a sinusoidal transverse load defined by

$$f^3(x_1, x_2) = \sin\left(\frac{\pi x_1}{L_1}\right), \tag{16}$$

where L_1 is the wavelength of the mechanical load in the x_1 direction.

The following displacement fields are used for the simply-supported plate example.

$$\vec{U} = \begin{cases} \begin{bmatrix} U_1(x^1, x^2, x^3) \\ U_2(x^1, x^2, x^3) \end{bmatrix} = u_\omega^n \begin{bmatrix} \phi_1^n \\ \phi_2^n \end{bmatrix} \cos px^1 \\ U_3(x^1, x^2, x^3) = u_3 \sin px^1. \end{cases} \tag{17}$$

Using the displacement field defined by equations (17), the following strain-displacement relations are obtained

$$\begin{aligned} \varepsilon_{11} &= -pu_\omega^n \phi_1^n \sin px^1 \\ \varepsilon_{22} &= 0 \\ 2\varepsilon_{12} &= -pu_\omega^n \phi_2^n \sin px^1 \\ 2\varepsilon_{13} &= (u_\omega^n \phi_{1,3}^n + pu_3)\cos px^1 \\ 2\varepsilon_{23} &= u_\omega^n \phi_{2,3}^n \cos px^1 \\ \varepsilon_{33} &= 0. \end{aligned} \tag{18}$$

The constitutive relations between stresses and strains for cord-rubber composite plates are given by the following relations as

$$\begin{bmatrix} \sigma_{11}^m \\ \sigma_{22}^m \\ \sigma_{33}^m \\ \sigma_{12}^m \end{bmatrix} = \begin{bmatrix} 2\mu_m + \lambda_m & \lambda_m & \lambda_m & 0 \\ \lambda_m & 2\mu_m + \lambda_m & \lambda_m & 0 \\ \lambda_m & \lambda_m & 2\mu_m + \lambda_m & 0 \\ 0 & 0 & 0 & 2\mu_m \end{bmatrix} \begin{bmatrix} \varepsilon_{11} \\ \varepsilon_{22} \\ \varepsilon_{33} \\ \varepsilon_{12} \end{bmatrix} \tag{19a}$$

$$\begin{bmatrix} \sigma_{13}^m \\ \sigma_{23}^m \end{bmatrix} = \begin{bmatrix} 2\mu_m & 0 \\ 0 & 2\mu_m \end{bmatrix} \begin{bmatrix} \varepsilon_{13} \\ \varepsilon_{23} \end{bmatrix}. \tag{19b}$$

For the cord, the following constitutive relations are used,

$$\begin{bmatrix} \sigma_{11}^c \\ \sigma_{22}^c \\ \sigma_{33}^c \\ \sigma_{12}^c \end{bmatrix} = \begin{bmatrix} C_{11}^c & C_{12}^c & C_{13}^c & 0 \\ C_{12}^c & C_{22}^c & C_{23}^c & 0 \\ C_{13}^c & C_{23}^c & C_{33}^c & 0 \\ 0 & 0 & 0 & C_{66}^c \end{bmatrix} \begin{bmatrix} \varepsilon_{11} \\ \varepsilon_{22} \\ 0 \\ \varepsilon_{12} \end{bmatrix} \tag{20a}$$

$$\begin{bmatrix} \sigma_{13}^c \\ \sigma_{23}^c \end{bmatrix} = \begin{bmatrix} C_{44}^c & 0 \\ 0 & C_{55}^c \end{bmatrix} \begin{bmatrix} \varepsilon_{13} \\ \varepsilon_{23} \end{bmatrix}. \tag{20b}$$

The cord coefficients are obtained using the Gough [3] and Tangaro [15] based on a homogeneous model.

The stress resultants used in the formulation are

$$\overline{P}_n^{\alpha} = \int_{-\frac{h}{2}}^{\frac{h}{2}} \sigma^{\alpha\beta} \phi_{\beta}^n dx^3;\ \overline{S}^{\alpha} = \int_{-\frac{h}{2}}^{\frac{h}{2}} \sigma^{\alpha 3} dx^3;\ \overline{Q}_n = \int_{-\frac{h}{2}}^{\frac{h}{2}} \sigma^{\alpha 3} \phi_{\alpha,3}^n dx^3;\ \overline{R}_1 = 0. \tag{21}$$

4.1. Example of one central cord layer plate

The first example is a one central cord layer distributed in the plate as described by Figure 4.

Figure 5 shows the first four in-plane transverse modes respectively in the $(\vec{x}_1, \vec{x}_3)$ and in the $(\vec{x}_2, \vec{x}_3)$ planes.

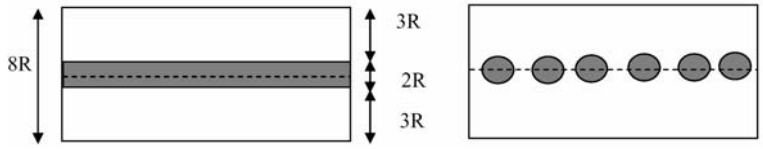

Figure 4. One central cord layer; d_c = 2.5h.

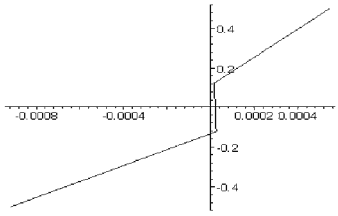

Normal mode number 1 in x_1 direction

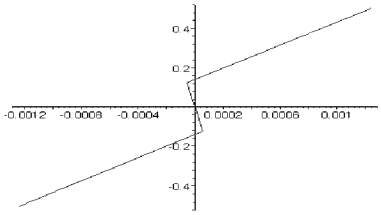

Normal mode number 1 in x_2 direction

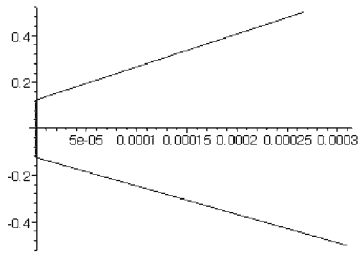

Normal mode number 2 in x_1 direction

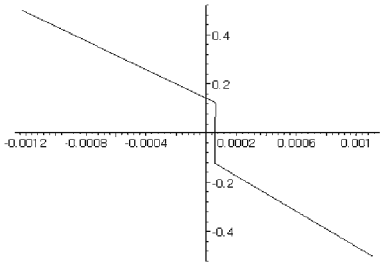

Normal mode number 2 in x_2 direction

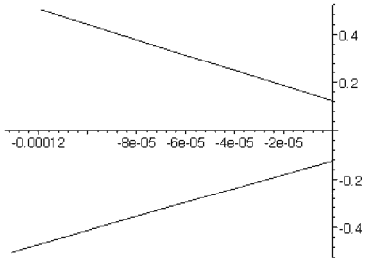

Normal mode number 3 in x_1 direction

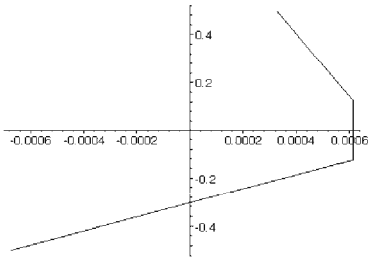

Normal mode number 3 in x_2 direction

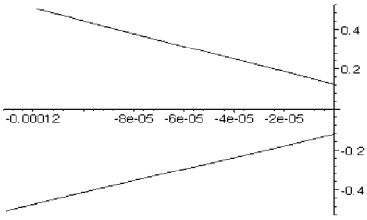

Normal mode number 4 in x_1 direction

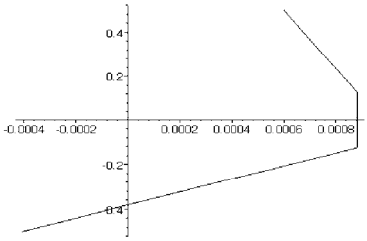

Normal mode number 4 in x_2 direction

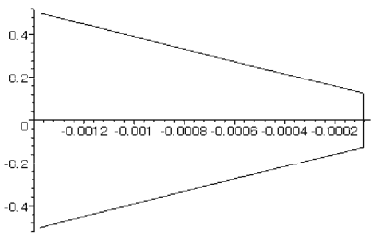

Normal mode number 5 in x_1 direction

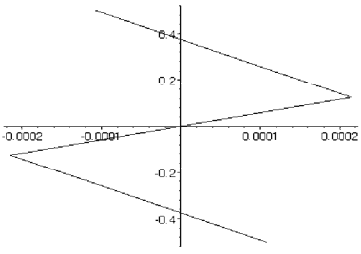

Normal mode number 5 in x_2 direction

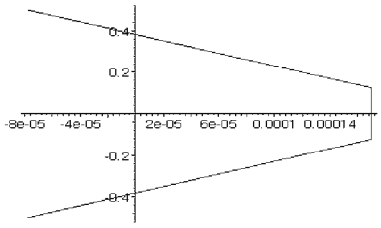

Normal mode number 6 in x_1 direction

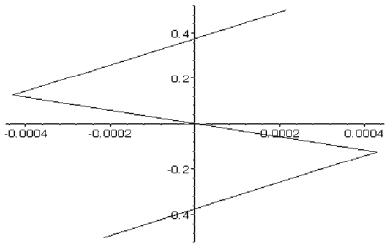

Normal mode number 6 in x_2 direction

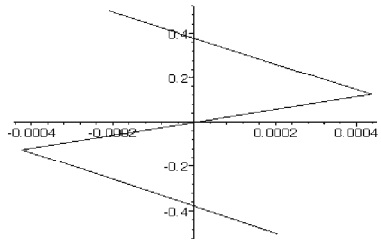

Normal mode number 7 in x_1 direction

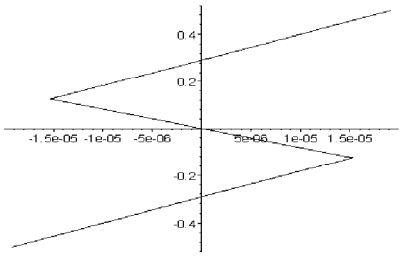

Normal mode number 7 in x_2 direction

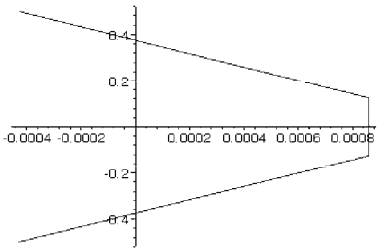

Normal mode number 8 in x_1 direction

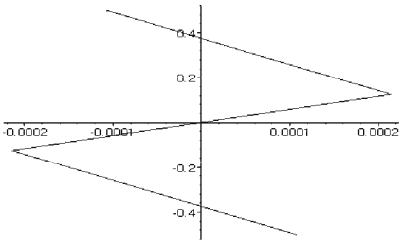

Normal mode number 8 in x_2 direction

Figure 5. The first eight normal modes associated to the system described by Figure 3.

The in-plane displacement and the normal stress are compared with the 2D equivalent model of Hassis and the exact solution of Pagano (without the coupling effect). In the solution of Pagano, three layers are considered: two matrix layers and one cord-matrix layer in which the Tangaro mechanical characteristics are considered, see Figure 6.

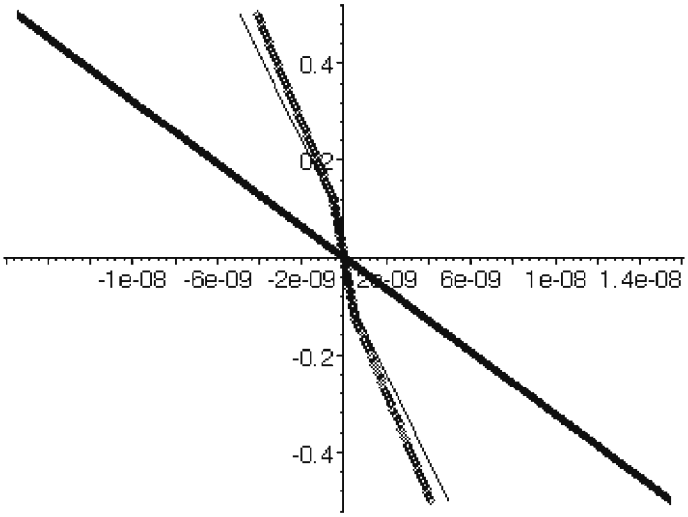

Figure 6(a). In-plan displacement U_1

(——) Pagano solution; (∘ ∘ ∘ ∘ ∘ ∘) Special warping solution; (—) 2D model of Hassis.

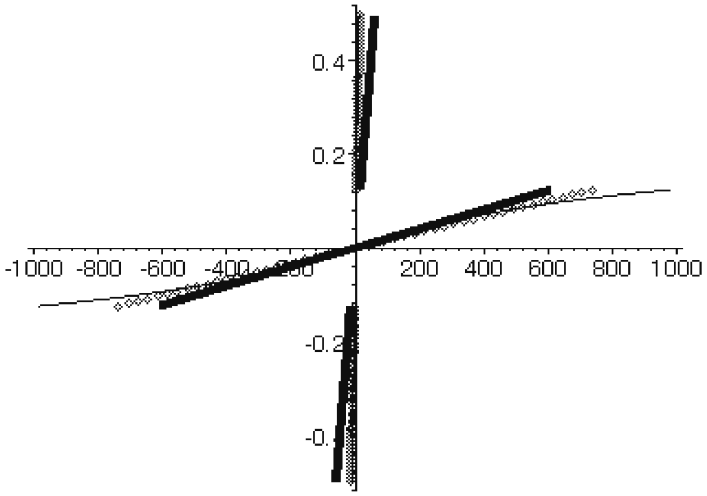

Figure 6(b). Normal stress σ_{11}

(——) Pagano solution; (∘ ∘ ∘ ∘ ∘ ∘) Special warping solution; (—) 2D model of Hassis.

4.2. Example of a two symmetrical cord layered plate

The second example considered is a two symmetrical cord layer distributed in the plate as shown in Figure 7.

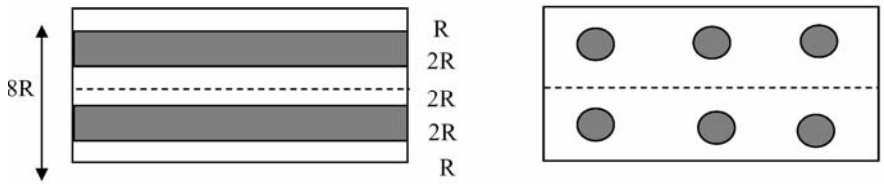

Figure 7. Two symmetrical cord layers; $x_3^1 = x_3^2 = 0.25\text{h}$; $d_c^1 = d_c^2 = 5\text{h}$.

The in-plane displacement and the normal stress are compared with the 2D equivalent model of Hassis and Pidaparti [4] and the exact solution of Pagano (without the coupling effect). In the solution of Pagano, three layers are considered: two matrix layers and one cord-matrix layer in which the Tangaro mechanical characteristics are considered, see Figure 8.

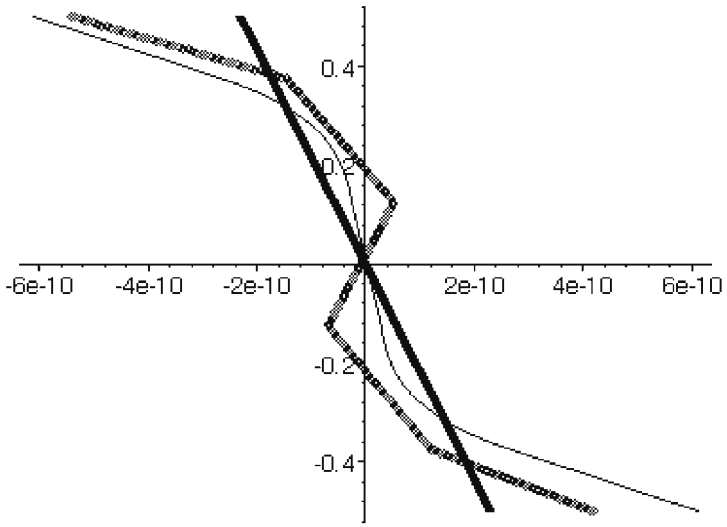

Figure 8(a). In-plane displacement U_1

(——) Pagano solution; (◦ ◦ ◦ ◦ ◦ ◦) Special warping solution; (▬▬) 2D model of Hassis.

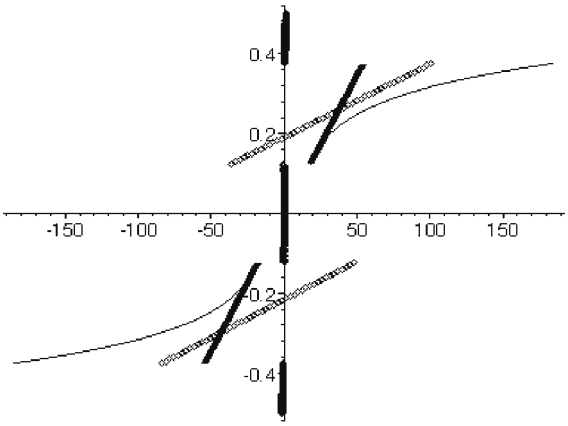

Figure 8(b). Normal stress σ_{11}

(——) Pagano solution; (◦ ◦ ◦ ◦ ◦ ◦) Special warping solution; (▬▬) 2D model of Hassis.

Figures 9(a-e) are plots of the in-plane displacement (U_1 and U_2) in the cord and in the matrix, the maximum normal stresses σ_{11} and σ_{22} for the cord and for the matrix, and the discontinuity of the normal stresses between cord and matrix, versus the ratio E_c/E_m.

5. Conclusion

The current investigation presents an analysis with a special warping model of laminated cord composite plates which takes into account of important coupling effects. The analytical formulation of the cord-rubber composite plates leading to the equilibrium equation and the boundary conditions is presented. The associated resultant stresses are defined and one layer and two layered cord-rubber composite plate examples are treated.

By comparing the results obtained with the homogeneous exact elasticity solutions of Pagano (without coupling between extension and twist), the two dimensional model of Hassis, it is obvious that the special warping high-order laminated plate theory gives a good approximation to the behaviour laminated plates. The in-plane contribution to the solution, the coupling extension - twist has been shown to be significant and

cannot be neglected. Thus, it is seen that for this kind of plates, a high order theory of the type special warping rather than classical models is required. In the case of the special warping model, there is no coupling between the in-plane and the out-plane responses. Due to the orthogonality of modes, the special warping model gives more simple equations than the homogeneous high-order models.

Due to the simplicity of the special modes (linear by layer), many numerical calculations become very easy and for numerical computer codes the theory presented here can be a powerful tool better than the homogeneous high-order theories.

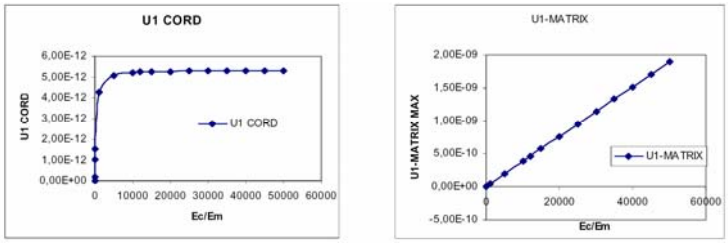

Figure 9(a). Maximum in plane displacement U_1 in the cord and in the matrix.

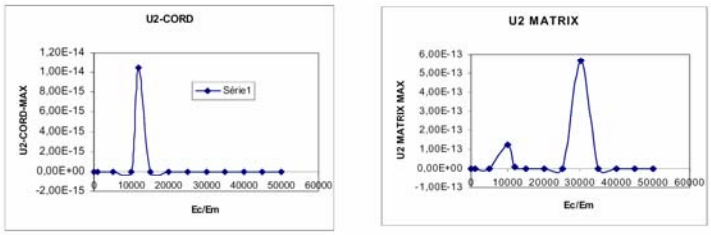

Figure 9(b). Maximum in plane displacement U_2 in the cord and in the matrix.

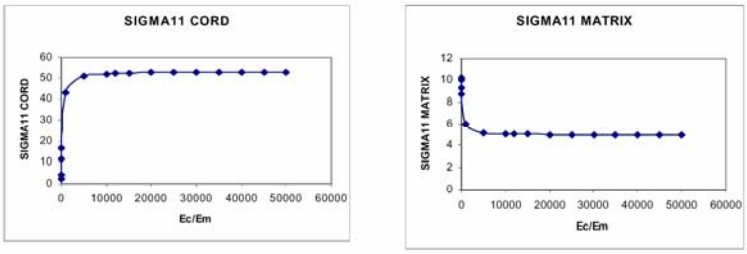

Figure 9(c). Maximum in plane stress σ_{11} in the cord and in the matrix.

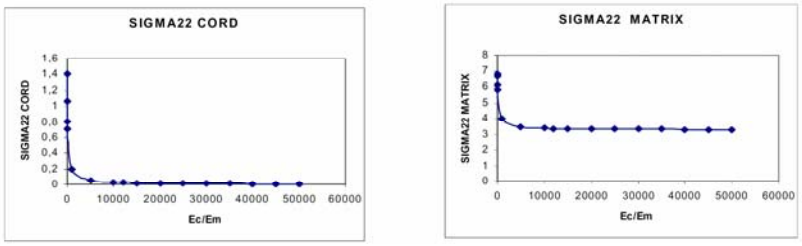

Figure 9(d). Maximum in plane stress σ_{22} in the cord and in the matrix.

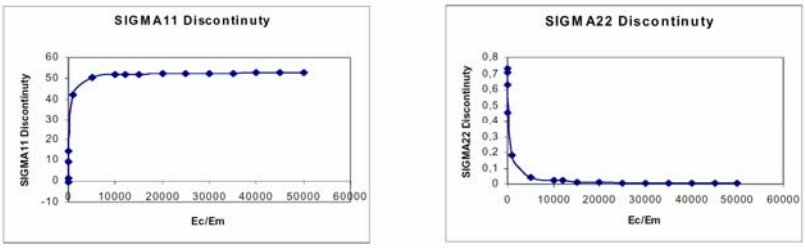

Figure 9(e). Discontinuity in plane stress σ_{11} and σ_{22} between the cord and the matrix.

Acknowledgement

The authors thank the U.S. National Science Foundation for supporting this work through grants INT-0096795 & 0504203.

References

[1] T. Akasaka and M. Hirano, Approximate elastic constants of fiber reinforced rubber sheet and its composite laminate, Composite Materials and Structures 1 (1972), 70-76.

[2] G. A. Costello, Theory of Wire Rope, Springer-Verlag, New York, 1990.

[3] V. E. Gough, Stiffness of cord and rubber constructions, Rubber Chemistry Technique 41 (1968), 988-1021.

[4] H. Hassis and R. M. Pidaparti, A two-dimensional general formulation for the cord-composite plates, Eur. J. Mech. A Solids 20 (2001), 811-826.

[5] S. Kocak and R. M. V. Pidaparti, Three-dimensional micromechanical modeling of cord-rubber composites, Mechanics of Advance Materials and Structures 7 (2000), 19-34.

[6] N. J. Pagano, Exact solutions for composite laminates in cylindrical bending, J. Comp. Mats. 3 (1969), 398-411.

[7] A. J. Paris and G. A. Costello, Bending of cord composite cylindrical shells, Journal of Applied Mechanics 67 (2000), 117-127.

[8] R. M. V. Pidaparti, Hierarchical Bending Analysis of Cord-Rubber Composites, AIAA J. 33 (1995), 2359-2363.

[9] R. M. V. Pidaparti, Analysis of cord-rubber composite laminates under combined tension and torsion loading, Composites Part B: Engineering 28 (1997), 433-438.

[10] R. M. V. Pidaparti, T. Y. Yang and W. Soedel, Modeling and fracture prediction of single ply cord-rubber composites, Journal of Composite Materials 26 (1992), 152-170.

[11] R. M. Pidaparti, S. Jayanti, J. Henkle and H. El-Mounayri, Design simulation of twisted cord-rubber structure using ProE/ANSYS, Composite Structures 52 (2001), 287-294.

[12] C. K. Shield and G. A. Costello, Bending of cord composite plates, Journal of Engineering Mechanics 120 (1994), 876-892.

[13] C. K. Shield and G. A. Costello, The effect of wire rope mechanics of the material properties of cord composites: an elastic approach, Journal of Applied Mechanics 61 (1996), 1-8.

[14] C. K. Shield and G. A. Costello, The effect of wire rope mechanics of the material properties of cord composites: an energy approach, Journal of Applied Mechanics 61 (1996), 9-15.

[15] G. Tangaro, Fiber-reinforced, oriented rubber sheets, Proc. Int. Rubber Conf., Moscow, Russia, 1968, pp. 459-466.